ZnO:Sn deposition by reactive evaporation: Effects of Sn doping on the electrical and optical properties.

Mr. Munguti L.K.
Kenyatta University
P.O. Box 43844
Nairobi-Kenya
mungutimunlak@yahoo.com

Dr Walter Njoroge
Kenyatta University
P.O. BOX 43844
Nairobi-Kenya
wanjoroge21@yahoo.co.uk

Dr Robinson J. Musembi
University of Nairobi
P.O. Box 30197
Nairobi-Kenya
musembirj@uonbi.ac.ke

Abstract: Tin doped zinc oxide thin films were deposited by reactive evaporation under various tin doping levels ranging from 1% to 8%. The deposition was done using Edwards Auto 306 coating unit at room temperature (25°C) and 5.0 x 10^{-5} mbar of chamber pressure. The optical transmittance spectra was obtained using UV-Vis-NIR spectrophotometer 3700 DUV in the visible wavelength 380-750nm. The doped films showed high transmittance >75% although slightly lower than that of undoped films. The band gap ranged from 2.95-3.95eV with the lowest value been attained at 4% tin doping. For the electrical characterization, sheet resistivity was carried using the four point probe at room temperature (25°C). The sheet resistivity ranged from 24.3-26.7Ωcm although it decreased with increase in doping concentration.

Keywords: Zinc oxide; Doping effects; Optical properties; Band gap.

I. INTRODUCTION

Zinc oxide is a II-VI semiconductor with a wide direct band gap [1] of 3.2 eV [2] at room temperature. Due to its high abundance and its non toxicity [3], it has a wide range of applications thus replacing the toxic indium tin oxide (ITO) as a transparent conducting oxide (TCO) for optoelectronic devices. It has large exciton binding energy of 60meV [3] which allows efficient excitonic emission at high temperatures. Moreover, its resistivity decreases due to doping[4], which has increased its use in gas sensors, varistors, UV-light emitters, transparent high power electronics, surface acoustic wave devices, piezoelectric transducers, gas sensing, solar cells and structural materials such as window material for display. Many methods have been employed to prepare ZnO thin films like spray pyrolysis [5], Molecular Beam Epitaxy [6], chemical vapor deposition [7], Pulse Laser Deposition PLD [8] and sol–gel [9]. The latest method has the advantage to give a high surface morphology at lower crystallizing temperature. Doping is a very useful way for turning ZnO to an electronic material. Many dopants such as group I, V and rare-earth elements have been used. Among those materials doping with Sn and Sb elements can result in interesting structural, optical and electrical properties optical since the Sb-doping may result in p-type conduction by the substituting of oxygen, on the other hand Sn constitutes a source of donor which introduces deep states in the band gap and results in reducing the gap [10]. In this study reactive thermal evaporation method was used in preparation the zinc oxide thin film.

II. EXPERIMENTAL

II. 1. Deposition of zinc oxide

Tin doped ZnO film was prepared from zinc granules and tin pellets. Zinc granules were 99.9% pure. Zinc was tin doped in various percentages by mass starting from 1% to 8%. This was done by calculations from the relative molecular mass of the compound. The various samples that were made are shown in table 2.1below.

Table 2.1: Tin doping level for Zinc Oxide

SAMPLE NAME	TIN DOPING LEVEL FOR ZnO
F	Undoped
G	1%
H	2%
I	3%
J	4%
K	5%
L	6%
M	7%
N	8%

Zinc granules were mixed with tin pellets as per the doping and heated in a sealed glass tube in presence of argon. The resulting alloy was cooled naturally to room temperature. The cooling was done in argon atmosphere for 10 minutes. The cooling time was recorded using a stop watch.

II.2. Deposition of tin doped zinc oxide (ZnO:Sn)

The sealed glass tubes were broken and the compound was removed. A mass of 0.1g of each sample was measured and placed in the boat of the evaporation chamber in the Edward's Auto 306 Coating unit evaporation system. The chamber was evacuated down to 5.0 $x10^{-5}$ mbar and oxygen was allowed at the rate 20 standard cubic centimetre (sccm). This reduced the chamber pressure to 4.8 x 10^{-5} mbar during the deposition period. The current of the heater filament in the chamber was maintained at 3.5A for 3 minutes. Since zinc is more reactive than tin, zinc oxide was formed. Microscope glass slides were used as substrate for all the film deposition. After the deposition all the samples were kept in microscope glass slides holder to prevent physical and or environmental damage.

III.3 Optical Properties

The raw data for the optical properties of both films were obtained using UV-VIS-NIR Spectrophotometer solid spec DUV at normal incidence. The data for each film was analyzed using the SCOUT software and graphs plotted using OriginPro7 software.

II.4. Electrical Characterization

The sheet resistivity measurements were carried out using the four point configuration at room temperature (25°C). The four point probe set up usually consists of four equally spaced tungsten metal tips with finite radius. Each tip is supported by springs on the other end to minimize sample damage during probing. The four metal tips are part of an auto-mechanical stage which travels up and down during measurements. A high impedance current source was used to supply current through the outer two probes and a voltmeter used to measure the voltage across the inner two probes as shown in figure 2. These values of sourced current and measured voltage were used to determine the sample resistivity. Typical probe spacing *S* was about 1 mm.

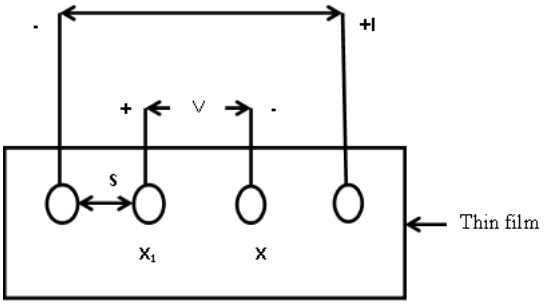

Figure 2.0: The four point probe linear set up.

2.5 *Elemental composition of the films.*

To determine the elemental composition of the films XRF spectroscopy was used. XRF spectroscopy is widely used for the qualitative and quantitative elemental analysis of environmental, geological, biological, industrial and other types of samples. Compared to some competitive techniques such as Atomic Absorption Spectroscopy (AAS), Inductively Coupled Plasma Spectroscopy (ICPS), and Neutron Activation Analysis (NAA), XRF has the advantage of generally being non destructive, multi-elemental, fast and cost effective. It also provides fairly uniform detection limit across a large portion of the periodic table and is applicable to a wide range of concentrations, from 100% to few parts per million. A main disadvantage is that analyses are generally restricted to heavier elements than fluorine.

III. Results and Discussion

III.1 Optical spectra of the films

The experimental data for transmittance and reflectance was obtained directly from UV VIS NIR Spectrophotometer DUV using the UVprobe software. The data was then converted in to Microsoft Office Excel format from which spectra graphs were plotted. The transmittance spectra for ZnO:Sn is shown in figure 3.1 below. The films showed high transmittance (>75%) in the visible region (380nm-780nm) showing that tin doped zinc oxide is a suitable window for solar cell applications. The films shows a sharp cut-off in the UV (<380nm) showing strong absorption property of the films. The doped films showed slightly lower transmittance compared with the undoped films in the same range. This can be attributed to the narrowing of the band gap and free charge carrier absorption of photons due increased levels of tin doping. In addition, at high doping levels, there is increased scattering of photons by crystal defects. The increase in transmittance with wavelength reduces beyond 800 nm. This is caused by increase in reflectance towards the infrared region. The transmittance for undoped films is higher than that of doped due to increased absorption in the doped films.

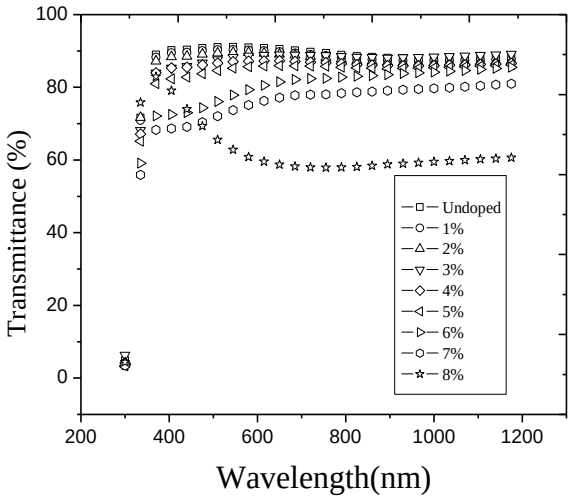

Figure 3.1: The transmittance spectra for tin doped zinc oxide.

III.2 Zinc oxide reflectance

Plots of spectral curves for ZnO:Sn thin films as shown in figure 3.2 shows that in visible spectrum range reflectance is generally low. For incident light of wavelengths above 1000nm, reflectance decreases greatly. This can be attributed to high transmission taking place as a result of low photon energy of incident light.

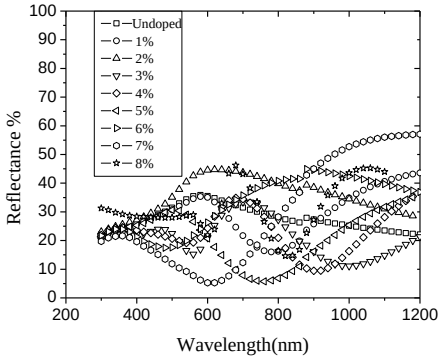

Figure 3.2: Optical reflectance of tin doped zinc oxide

From the plot in figure 5.15, the visible range is characterized by undulating curves with maximum and minimum points. These points are associated with interband transition where electrons from filled states at the top of valence band absorb incident photon energy almost equal to energy band gap and thus photo-excited to empty states in the conduction band. The points are attained within energy range which corresponds with the energy band gaps of the thin films. These photo-transitions at low energy ranges are caused due to fundamental absorption.

The figure 3.3 below shows the fittings of the experimental and simulated data for various samples of tin doped zinc oxide.

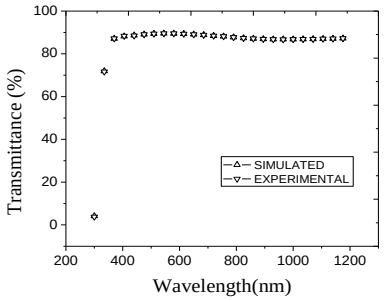

Figure 3.3: Simulated versus experimental graph for zinc oxide doped at 4% tin concentration.

The diagrams below shows a plot of $(\alpha hv)^2$ against energy(eV). The extrapolation of the linear part of the curve to the energy axis $\left\{(\alpha h\nu)^2 = 0\right\}$ gives the energy gap E_g.

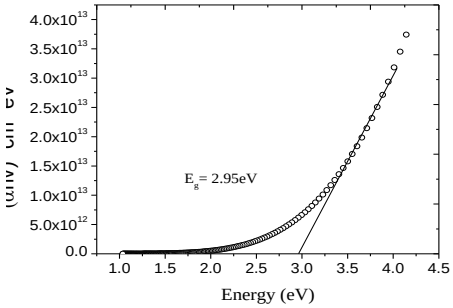

Figure 3.4: Extrapolation of the linear part of $(\alpha hv)^2$ against energy(eV)for tin doped zinc oxide. The band gap energy was obtained was 2.95 eV for 4% tin concentration.

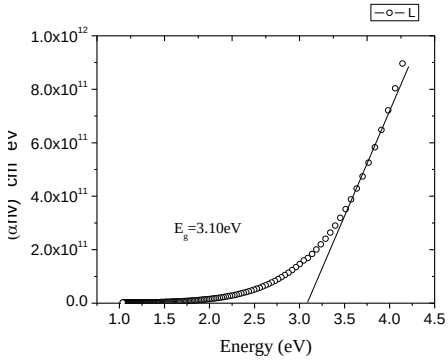

Figure 3.5: Extrapolation of the linear part of $(\alpha hv)^2$ against energy(eV)for tin doped zinc oxide. The band gap energy was obtained was 3.10 eV for 3% tin concentration.

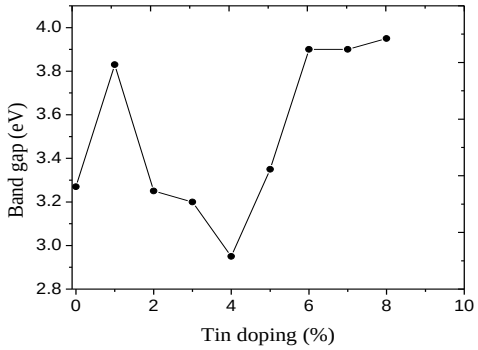

Figure 3.6: Variation of band gap with tin doping concentration. The lowest band gap was obtained at 4% tin doping.

The graph in figure 3.6 shows that the band gap decreases with increase in tin doping reaching the lowest value at 2.95eV at 4%. Further tin doping leads to increase in band gap at the doping concentration of more than 4%. It is attributed to the fact that the excess tin atoms were segregated into the grain boundaries at the doping concentration of more than 4%. These segregated tin atoms did not act as dopants.

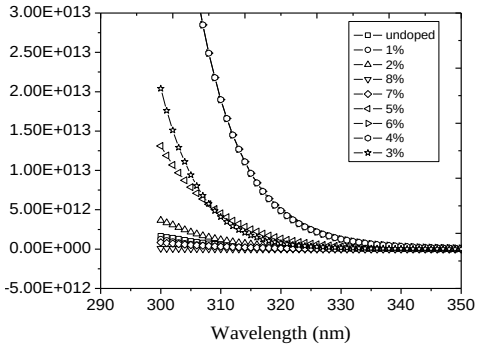

Figure 3.7: *Absorption coefficient of tin doped zinc oxide.* Low absorption coefficient indicates that zinc oxide is a good window layer for solar cells.

At high wavelengths, absorption was low as shown in figure 3.7. This was an indication that the film is optically transparent to photons incident on its surface. However at small wavelengths absorption coefficients are high since absorption of incident photon takes place. There was an increase in absorption for films between 3% and 5% tin doping concentration. This can be attributed to increase in charge carriers due to doping. However for high concentration of tin doping the dopant atoms are bound by strong electric field and thus the charge carriers are unable to absorb photons.

III.3 Electrical resistivity for ZnO:Sn film

Electrical resistivity's of ZnO and ZnO:Sn for various doping concentrations were measured and presented in graph on figure 3.8. The thickness of the films was of the range 90–150nm.

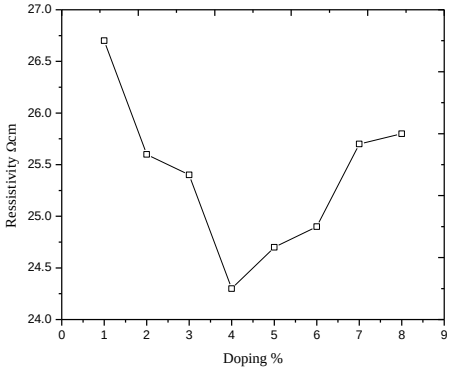

Figure 3.8: Variation of resistivity with the tin doping levels.

Resistivity of undoped ZnO decreases sharply with 1% tin doping. The lowest resistivity was reached at 4% tin doping. The decrease in resistivity may be explained as follows: since the ionic radius of tin (0.38 °A) is smaller than that of the zinc ion (0.6 °A), the tin atoms doped into a ZnO lattice act as donors by supplying two free electrons when the Sn ions occupy Zn ion sites. This in turn increases the free carrier concentration and hence

decreases the resistivity. The mechanism of the conduction can be described by the (3.0) below;

$$SnO_{2\,ZnO} \rightarrow Sn''_{Zn} + O_0^x + \frac{1}{2}O_2 + 2e' \qquad (3.0)$$

Sn^{4+} ions substituted Zn^{2+} ions in the lattice induce positive Sn''_{Zn} charges in the material. In order to maintain electrical neutrality, two negative electrons are induced to compensate the excess positive charges. Hence the resistivity decreases due to increasing free electrons in the film. In the concentrations between 1% and 4% of Sn dopants, little decrease of resistivity is found. However, when more than 4% of Sn was added, the resistivity gradually increased. At higher concentrations more tin atoms can be effectively incorporated into the lattice of ZnO. On the other hand, the residual stress arises simultaneously as well. The stress field would reflect electric carriers and result in high resistivity. Further more as the doping level is increased, more dopant atoms Zn atoms in the crystal grain and grain boundaries tend to saturation. In this case over high doping concentration will lead to large quantity of ionized impurity. The ionized impurity provide strong scattering centres for charge carriers [10]. According to the Conwell-Weisskoft formula, when degenerate charge carriers are scattered by impurity ions, the energy dependence of ionized impurity scattering mobility μ_i is:

$$\mu_i = \frac{e}{m^*}\tau_i(E_F) = \left(\frac{2}{m^*}\right)^{\frac{1}{2}} \frac{\varepsilon^{\frac{1}{2}} E_F^{\frac{3}{2}}}{\Pi e^3 N_i Z^2} \frac{1}{\ln\left(1 + \frac{\varepsilon E_F}{N_i^{\frac{1}{3}} Z e^2}\right)} \qquad (3.1)$$

Where $\tau_i(E_F)$ is the relaxation time, which takes into account the scattering events occurring near the Fermi level E_F, ε is the static dielectric constant of the film, *m** is the effective mass of electrons, *Ze* is the ion charge and *Ni* is the concentration of the scattering centres. From the equation above we can see that a high doping concentration will lead to a large quantity of ionized impurity, resulting to decrease in mobilities of the ZnO:Sn films.

III.4 XRF spectrum for tin doped zinc oxide (ZnO:Sn)

XRF analysis was carried out using MiniPal2 XRF machine which analyses heavy materials. The analysis was carried out to ascertain the elemental composition of the thin films. The analysis is peak-based where elemental intensities of thin films are calculated and respective spectral background obtained. In figure 3.9, the XRF spectrum for ZnO:Sn shows the peaks of elemental composition of the film.

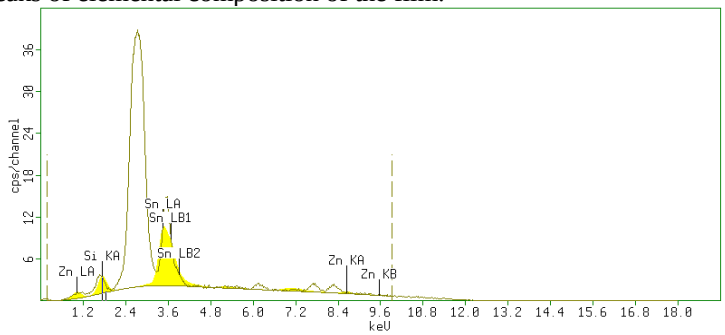

Figure 3.9: *XRF spectrum of ZnO:Sn thin film* with 4% Sn doping concentration.

The shaded peaks are the elemental composition of the thin film. The elements detected from the XRF analysis are Zn (15%) and Sn (85%) as seen from coloured peaks. For Zn peaks were detected at energies of 1.18 keV, 8.42 keV and 9.6 keV. Peak X is the detector escape which is a spectrum for detector peak. The MiniPal2 XRF machine used filters the detector escape but its spectrum display remains, a reason why it is faint. The faint spectral line Y at the bottom is for the background radiation which is also filtered but remains displayed.

IV. Conclusion

IV.1 Conclusion

Deposition of thin films of ZnO:Sn was done by reactive thermal evaporation technique. The transmittance data of the films were measured and the films were found to have a high transmittance of above 75 % within the visible range. The optical band gap obtained ranged between 2.95eV and 3.95eV. It was also observed that the band gap decreased with increase in the doping concentration reaching an optimum at 4% tin doping. Although the absorption coefficient for tin doped zinc oxide thin films was low the highest absorption was noted for the films between 3% and 5% doping concentration. It was also noted that the resistivity of tin doped zinc oxide reached its lowest value of 23.4Ωcm at 4% doping level.

Acknowledgement

The authors of this work want to thank the Chief Geologist Department of Mines and Geology Ministry of Environment and Natural Resources for the use XRF spectrometer.

References

[1] Sundaram, K.B. and Khan, A. (1997). "Characterization and optimization of zinc oxide films by r.f. magnetron sputtering". *Thin Solid Films.* **295:** 87-91

[2] Norton , D.P., Ivill, M., Li Y., Kwon,Y.W., Erie, J.M., Kim, H.S., Ip K., Pearton, S.J., Heo,Y.W., Kim, S., Kang, B.S., Ren, F., Hebard, A.F. and Kelly, J., (2006). "Charge carrier and spin doping in ZnO thin films". *Thin Solid Films* **496:** 160 – 168

[3] Hisao, M., Naoki, Y., Aki, M., Takahiro, Y., Yoshinori, H., Hiroaki, I., Takahiro, I., Hitoshi, H.C., Hisashi, A.C., Tetsuya, Y. (2009). "Influence of thermal annealing on electrical and optical properties of Ga-doped ZnO thin films". *Thin Solid Films* **518:** 1386–1389

[4] Vaezi, M. and Sadrnezhaad, S. (2007). "Improving the electrical conductance of chemically deposited zinc oxide thin films by Sn dopant". *Material Science Engineering*, **141:** 23-27

[5] Benny J, Gopchandran, K.G., Manoj, P.K., Koshy, P., and Vaidyan V.K., (1999). "Optical and electrical properties of zinc oxide films prepared by spray pyrolysis". *Bull Mater Sci* **22(5):**921–6.

[6] Xiu, F.X., Yang, Z., Mandalapu, L.J., Zhao, D.T. and Liua, J.L. (2005). "High-mobility Sb-doped *p*-type ZnO by Molecular-Beam -Epitaxy". *Applied Physics Letters.* **87:** 152101

[7] Funakubo. H., Mizutani, N.,Yonetsu, M,., Saiki, A., and Shinozaki, K. (1999). "Orientation control of ZnO thin film prepared by CVD". *J Electroceram* **4:**25–32.

[8] Shan, F.K., Shin, B.C., Kim, S.C. and Yu, Y.S. (2003). "Substrate effect of ZnO thin films prepared by Pulse Laser Deposition (PLD)". *J. Eur. Cerm. Soc*. **24:** 1015-1018.

[9] Benelmadjat, H., Boudine, B., Halimi, O. and Sebais, M. (2009). "Fabrication and chacterization of pure and Sn/Sb-doped ZnO thin films deposited by sol-gel method". *Optics and Laser Technology*. **41:** 630-633

[10] Vaezi, M. and Sadrnezhaad, S. (2007). "Improving the electrical conductance of chemically deposited zinc oxide thin films by Sn dopant". *Material Science Engineering*, **141:** 23-27